UNIVERSITY OF
BATH

Citation for published version:
Johnston, N, Pan, M, Plummer, A, Hillis, A & Yang, H 2015, 'Theoretical Studies of a Switched Inertance Hydraulic System in a Four-Port Valve Configuration' Paper presented at The Seventh Workshop on Digital Fluid Power, Linz, Austria, 26/02/15 - 27/02/15, .

Publication date:
2015

Document Version
Early version, also known as pre-print

Link to publication

University of Bath

THEORETICAL STUDIES OF A SWITCHED INERTANCE HYDRAULIC SYSTEM IN A FOUR-PORT VALVE CONFIGURATION

Nigel Johnston[1], Min Pan[2], Andrew Plummer[1], Andrew Hillis[1], Huayong Yang[2]

1. Centre for Power Transmission and Motion Control, University of Bath, BA2 7AY, UK
2. The State Key Lab of Fluid Power Transmission and Control,
Zhejiang University, 310027, China
E-mail: D.N.Johnston@bath.ac.uk

ABSTRACT

A switched inertance hydraulic system (SIHS) can provide an efficient step-up or step-down of pressure or flow rate by using a digital control technique. In this article, analytical models of a SIHS in a four-port high-speed switching valve configuration are proposed, and system characteristics and performance are studied. Using these models, the flow responses, system characteristics and efficiency can be estimated and investigated effectively and in detail. Numerical simulation models are used in validation of the analytical models. Results show that the models are accurate and reliable, and give a very promising way to understand the characteristics and trend of a four-port switched hydraulic system. A discussion and comparison is included of the three-port valve and four-port valve configurations, in terms of system power loss. It is found that the four-port configuration has higher losses, but provides greater control flexibility.

KEYWORDS: Digital hydraulics, Switched inertance hydraulic systems, Four-port switching valves, Efficient fluid power;

1 INTRODUCTION

A switched inertance hydraulic system, which performs analogously to an electrical 'switched inductance' transformer, is one possible approach to raise the efficiency of hydraulic systems [1-3]. This technique makes use of the inherent reactive behaviour of hydraulic components. A fluid volume can have a capacitive effect, whilst a small

diameter line can have an inductive effect [1]. This also requires high-speed switching valves to achieve sufficiently high switching frequencies with fast transitions, and to minimize the pressure and flow loss at the valve orifices. The valve ideally should have low resistance and low leakage and be able to operate with a very fast switching frequency [4-6]. Effective analytical models which are able to describe the system effectively in equations and easily present the relationship of the switching parameters (switching frequency and ratio), system parameters (valve resistance, tube length and diameter) and system efficiency are needed. Some recent work has been done for this, but most research focused on the SIHS in a three-port valve configuration [7-11]. This article presents analytical models of a SIHS in a four-port valve configuration, which provide effective tools to analyse the effects of system parameters and investigate the physical characteristics of four-port switched devices.

Two-port flow control valves are capable of modulating flow and pressure in one direction but do not generally provide for reversal of direction of the load. However four-port modulating valves and servovalves provide the capability to reverse the direction of motion or force smoothly through the same control action, providing true four-quadrant operation and seamless changes in direction. They also provide a combination of meter-in and meter-out control which is generally safe under over-running load conditions. Most hydraulic motion control systems use four-port valves for these reasons. However because four-port valves effectively provide two restrictions in series, one upstream and one downstream of the load, the overall resistance is higher than that of a two-port valve. Cross-port leakage can also occur.

The SIHS can be configured to operate as a four-port control device in a similar way to a four-port proportional valve [1, 2]. Figure 1 shows the configuration of a four-port control device [12]. It consists of a high-speed four-port switching valve with two common ports A and B, two switched ports and two long, small diameter inertance tubes. The common port A is connected alternately to the high pressure supply port and then low pressure supply port, whilst the common port B is connected synchronously to the low pressure supply port then high pressure supply port. This can be also named as a 'push-pull' configuration, where two inertance tubes are used and can be considered as a combination of two three-port valve configurations with the same delivery flow in the opposite directions [1, 2, 12]. The switching valve operates cyclically and rapidly such than the high and low pressures are opened alternately. The delivery port might connect to a loading system and includes capacitance such that the load pressure is approximately constant.
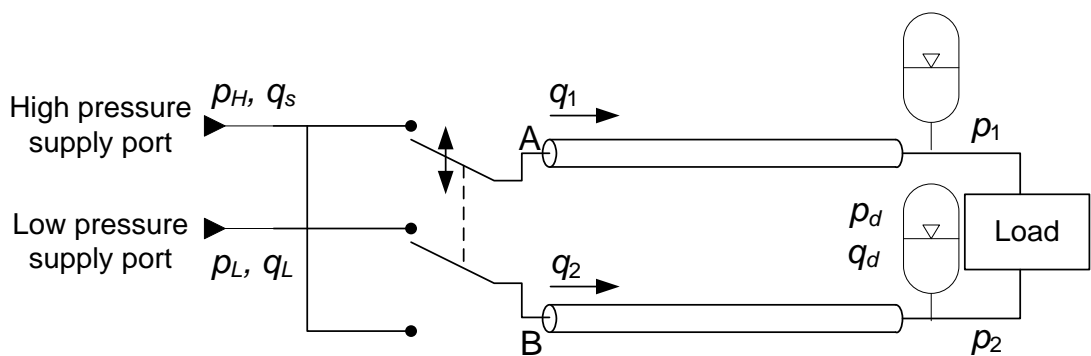

Fig. 1: Four-port valve configuration [1, 2, 12]

A typical pulsed switching signal and the flow responses in the two tubes for ideal operation are shown in Figure 2.
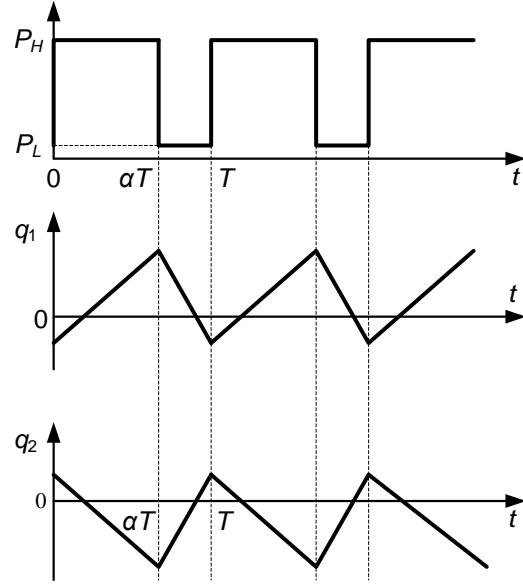

Fig. 2: Typical ideal switching pressure and flow responses [2]

Theoretically, for ideal operation with 100% efficiency and no losses, the relationship between the delivery pressure and the supply pressure of a four-port valve configuration is given by Equation (1), where α is the switching ratio [2].

$$p_d = p_1 - p_2 = (p_H - p_L)(2\alpha - 1) \tag{1}$$

which can be seen as the pressure difference between p_1 and p_2. The output pressure is proportional to the input pressure difference.

The delivery can be given by Equation (2) and (3) [2].

$$q_d = \frac{1}{2\alpha - 1} \bar{q}_H \tag{2}$$

$$q_d = \frac{1}{1 - 2\alpha} \bar{q}_L \tag{3}$$

where the delivery flow q_d comes partly from the low pressure supply port, and is higher than the high pressure port flow $\bar{q}_H$. From Equation (1-3), it also can be seen that ideally zero delivery pressure and supply flow occur when the switching ratio α is 0.5.

2   LUMPED PARAMETER MODEL

The lumped parameter model simplifies the description of the behaviour of the distributed physical system into a system consisting of discrete entities that approximate the behaviour of distributed system under certain assumptions.

For laminar flow in the pipeline, the lumped parameter model takes the form of a series of lumped parameter resistor/inductor/capacitor (RLC) networks [13]. It is a simple method to implement and is very flexible in that variable properties and cavitation can be included. It also has been successfully proved in the analysis of SIHS in a three-port configuration. In this section, the lumped model of a SIHS in a four-port configuration was studied as shown in Figure 3.
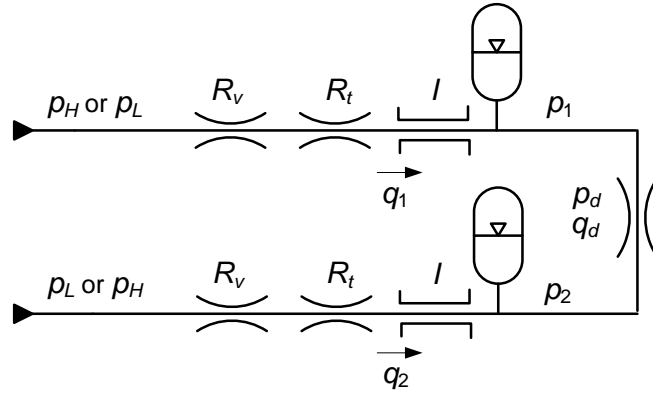
Fig. 3: Lumped parameter model for a SIHS in a four-port configuration

The following assumptions are made.

- The supply pressures, p_H and p_L, and the delivery pressures p_1, p_2 and p_d are constant;
- The high-pressure and low-pressure supply ports of the switching valve have the same resistance R_v;
- Switching occurs instantaneously;
- The valve resistance R_v is linear and time-invariant;
- The two tubes are identical;
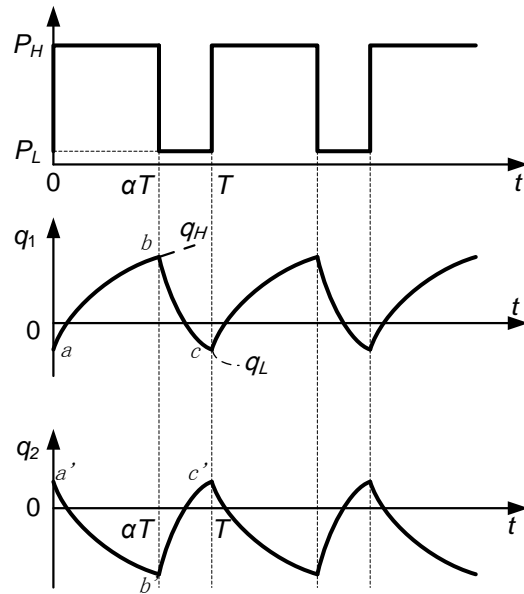- There is no valve leakage across the ports.

Fig. 4: Typical switching pressure and flow responses with system resistances

Including system resistances, the supply pressure and flow rates from the high and low-pressure supply ports are shown in Figure 4. Referring to the previous work [8, 9], the laminar flow rate q_1 and q_2 can be described as:

$$q_1(t) = \begin{cases} \dfrac{(p_H - p_L)(\alpha - \alpha \cdot e^{\frac{T}{\tau}} + e^{\frac{T}{\tau}} + e^{\frac{-t-\alpha \cdot T}{\tau}} - e^{\frac{-t+T}{\tau}} - 1)}{(e^{\frac{T}{\tau}} - 1) \cdot R} + q_d & 0 \le t \le \alpha T \\[4mm] \dfrac{(p_H - p_L)(\alpha \cdot e^{\frac{T}{\tau}} + e^{\frac{-t+T}{\tau}} - e^{\frac{-t+\alpha T+T}{\tau}} - \alpha)}{(1 - e^{\frac{T}{\tau}}) \cdot R} + q_d & \alpha T \le t \le T \end{cases} \tag{4}$$

$$q_2(t) = -q_1(t) \tag{5}$$

where R is the overall system resistance, $R = R_v + R_t$.

The average flow rate from the high-pressure supply port $\bar{q}_H$ corresponds to the integral of Equation (4) through the one switching period divided by T, as shown in Equation (6).

$$\bar{q}_H = \frac{V_{ab} + V_{b'c'}}{T} = \frac{\int_0^{\alpha T} q_1(t)dt + \int_{\alpha T}^T q_2(t)dt}{T} \tag{6}$$

Thus,

$$\bar{q}_H = \frac{2\tau(e^{\frac{-\alpha T}{\tau}} - e^{\frac{\alpha T}{\tau}} + e^{\frac{T}{\tau}} - e^{\frac{-T}{\tau}} + e^{\frac{-T(1-\alpha)}{\tau}} - e^{\frac{T(1-\alpha)}{\tau}})(q_H - q_L)}{(2 - e^{\frac{T}{\tau}} - e^{\frac{-T}{\tau}})T} + q_H \alpha - q_L(1-\alpha) \tag{7}$$

where $q_H = \dfrac{p_H - p_d}{R}$ and $q_L = \dfrac{p_L - p_d}{R}$.

As the previous research stated [8, 9, 14], normally the actual average flowrate from the high pressure supply port $\bar{q}_H$ is higher than the ideal average flowrate $q_d(2\alpha - 1)$, and the average flowrate from the low pressure supply port is lower than the ideal average flowrate $q_d(1 - 2\alpha)$. Therefore, system flow loss can be defined as:

$$q_{loss} = \bar{q}_H - q_d(2\alpha - 1) \tag{8}$$

or

$$q_{loss} = q_d(1 - 2\alpha) - \bar{q}_L \tag{9}$$

Substituting Equation (7) into Equation (8), the flow loss represented in the time domain can be given by Equation (10).

$$q_{loss-t} = 2\frac{\tau(e^{\frac{-\alpha T}{\tau}} - e^{\frac{\alpha T}{\tau}} + e^{\frac{T}{\tau}} - e^{\frac{-T}{\tau}} + e^{\frac{-T(1-\alpha)}{\tau}} - e^{\frac{T(1-\alpha)}{\tau}}) + \alpha T(1-\alpha)(2 - e^{\frac{T}{\tau}} - e^{\frac{-T}{\tau}})}{(2 - e^{\frac{T}{\tau}} - e^{\frac{-T}{\tau}})TR}(p_H - p_L)$$

$$\tag{10}$$

This shows that the flow loss is affected by the pressure difference, but not directly affected by the delivery flowrate, which is similar to the flow loss in the three-port configuration [8, 9].

Regarding the system pressure, the pressure p_1 can be represented as:

$$p_1 = p_H \alpha + p_L(1 - \alpha) - q_d R \tag{11}$$

and the pressure p_2 is:

$$p_2 = p_H(1-\alpha) + p_L\alpha + q_dR \tag{12}$$

The actual delivery pressure difference is:

$$p_d = p_1 - p_2 = (p_H - p_L)(2\alpha - 1) - 2Rq_d \tag{13}$$

which shows the relationship of delivery pressure, supply pressures and delivery flowrate. The actual delivery pressure is the difference between the ideal delivery pressure as shown in Equation (1) and the pressure loss due to resistance with a fixed system overall resistance R.

The pressure loss of a four-port configuration thus can be calculated as:

$$p_{loss} = 2Rq_d \tag{14}$$

Alternatively, the laminar flow rate q_1 and q_2 can be also described in the frequency domain [8, 9]. Taking the Fourier transform of the supply pressure p_H and p_L, the Fourier coefficient P_n is:

$$P_n = \frac{p_H}{2\pi nj}(1 - e^{-j2\pi n\alpha}) + \frac{p_L}{2\pi nj}(e^{-jn2\pi\alpha} - e^{-jn2\pi}) \tag{15}$$

The Fourier coefficient Q_n of the flowrate is given by using Equation (16),

$$Q_n = \frac{P_n}{Z_E} \tag{16}$$

where Z_E is the system impedance which is the ratio of the pressure ripple to the flow ripple at the entry to the hydraulic circuit [15]. For a lumped parameter model, the entry impedance Z_E can be described by Equation (17):

$$Z_E = R + j\omega I \tag{17}$$

Substituting Equation (15) and (17) to Equation (16),

$$Q_n = \frac{p_H(1 - e^{-j2\pi n\alpha}) + p_L(e^{-jn2\pi\alpha} - e^{-jn2\pi})}{-2\pi njR - 2\pi n\omega I} \tag{18}$$

Using Fourier series, the supply dynamic flow rate $q_1(t)$ and $q_2(t)$ in the time domain can be obtained:

$$q_1(t) = 2\sum_{n=0}^{\infty} Q_n e^{\frac{jn2\pi \cdot t}{T}} + q_d \tag{19}$$

$$q_2(t) = -q_1(t) \tag{20}$$

The average flow rate from the high-pressure port can be represented as:

$$\bar{q}_H = \frac{\int_0^{\alpha T} 2\sum_{n=0}^{\infty} Q_n e^{\frac{jn2\pi \cdot t}{T}} dt - \int_{\alpha T}^{T} 2\sum_{n=0}^{\infty} Q_n e^{\frac{jn2\pi \cdot t}{T}} dt}{T} + q_d(2\alpha - 1) \tag{21}$$

$$= -2\sum_{n=0}^{\infty} \text{Re}\left[\frac{Q_n}{2\pi nj}(1 - e^{jn2\pi\alpha})\right] - 2\sum_{n=0}^{\infty} \text{Re}\left[\frac{Q_n}{2\pi nj}(e^{jn2\pi} - e^{jn2\pi\alpha})\right] + q_d(2\alpha - 1)$$

The flow loss based on the frequency-domain calculation can be obtained as:

$$q_{loss-f} = -2\sum_{n=0}^{\infty}\text{Re}\left[\frac{Q_n}{2\pi n j}(1-e^{jn2\pi\alpha})\right] - 2\sum_{n=0}^{\infty}\text{Re}\left[\frac{Q_n}{2\pi n j}(e^{jn2\pi}-e^{jn2\pi\alpha})\right] \quad (22)$$

The upper limit of the summation can be chosen to give a finite number of harmonics. 100 harmonics were considered and used for the following calculations. The frequency-domain calculation gives virtually identical results to the time-domain calculation; however it provides additional flexibility as it ca be extended to a distributed parameter pipeline mode as shown below.

3   DISTRIBUTED PARAMETER MODEL

For the distributed parameter model, the entry impedance Z_E is given by Equation (23):

$$Z_E = jZ_0\xi\tan(\frac{\omega L\xi}{c}) + R_v \quad (23)$$

where $Z_0 = \rho c/A$ is the pipe characteristic impedance, R_v is the valve resistance and ξ is the viscous wave correction factor [16].

$$\xi = \left(1-\frac{2}{z}\frac{J_1(z)}{J_0(z)}\right)^{-\frac{1}{2}} \text{ and } z = jr\sqrt{\frac{j\omega}{\nu}} \quad (24)$$

Substituting Equation (23) into Equation (16), the Fourier coefficients Q_n are given by Equation (25).

$$Q_n = \frac{p_H(1-e^{-j2\pi n\alpha}) + p_L(e^{-jn2\pi\alpha}-e^{-jn2\pi})}{2\pi n j(jZ_0\xi\tan(\frac{\omega L\xi}{c}) + R_v)} \quad (25)$$

Using equation (19) and (20), the supply dynamic flow rate $q_1(t)$ and $q_2(t)$ can be calculated based on the distributed parameter model. Also, the average flow rate from the high-pressure port $\bar{q}_H$ and the flow loss can be obtained by using equations (21) and (22).

4   SYSTEM POWER LOSS AND EFFICIENCY

The input power of the system can be given by Equation (26),

$$P_{in} = \bar{q}_H p_H + \bar{q}_L p_L = \bar{q}_H(p_H - p_L) \quad (26)$$

The system power loss can be obtained by using Equation (27),

$$P_{loss} = \bar{q}_H(p_H - p_L) - q_d p_d = q_{loss}(p_H - p_L) + 2Rq_d^2 \quad (27)$$

which shows the system power loss in a four-port configuration is influenced by the system flow loss, supply pressure difference, delivery flow rate and resistance.

The system efficiency can be described as:

$$\eta = \frac{q_d(2\alpha-1)(p_H - p_L) - 2Rq_d^2}{q_{loss}(p_H - p_L) + q_d(2\alpha-1)(p_H - p_L)} \times 100\% \quad (28)$$

or

$$\eta = \left(1 - \frac{q_{loss}}{\overline{q}_H} - \frac{p_{loss}q_d}{\overline{q}_H(p_H - p_L)}\right) \times 100\% \qquad (29)$$

which shows the relationship of the system efficiency, flow loss and pressure loss. When the load is negative, the regenerative efficiency is defined as [1]:

$$\eta' = \frac{1}{\eta} \times 100\% \qquad (30)$$

5 SIMULATION

A time-domain numerical simulation model was created using MATLAB Simulink, using conventional numerical integration techniques. The high-speed switching valve was assumed to switch instantaneously and was modelled with a constant linear resistance of 20 bar/(L/s). The inertance tube was represented by a lumped parameter model and a distributed parameter model, respectively. The inertance in the lumped parameter model is given approximately by Equation (31), neglecting viscous and end effects and assuming a uniform velocity profile over the cross-section. The resistance, assuming fully developed laminar flow, is given by Equation (32) in the lumped parameter model.

$$I = \frac{4\rho L}{\pi d^2} \qquad (31)$$

$$R = \frac{128\rho \nu L}{\pi d^4} \qquad (32)$$

A distributed parameter model assumes that the attributes of the circuit, such as resistance, capacitance and inertance, are distributed continuously throughout the circuit. This is in contrast to the common lumped parameter model [11]. The Transmission Line Method (TLM) was used to model the wave propagation in the inertance tubes. The model was developed by Krus et al [17] and modified by Johnston [18, 19] to include unsteady or frequency-dependent friction. The TLM model accurately and efficiently represents wave propagation and laminar friction over a very wide frequency range. A small compressible volume (5 cm^3) was included between the valve model and the TLM inertance tube model. Parameters for the analytical lumped and distributed parameter models and simulation models in Simulink are listed in Table 1.

Table 1: Parameters for analytical four-port SIHS and simulation

Resistance of high-speed switching valve R_v	20 bar/(L/s)
Length of two tubes L_1 and L_2	1 m
Diameter of tube d	10 mm
Speed of sound c	1350 m/s
Average delivery flowrate q_d	1 L/s
High supply pressure p_H	100 bar
Low supply pressure p_L	10 bar
Switching frequency f	100 Hz
Switching ratio α	0.7
Density ρ	870 kg/m^3
Viscosity ν	32 cSt

Figure 5 (a) shows a comparison of the results from the lumped parameter simulation model and the proposed analytical time-domain lumped model. The analytical frequency domain lumped model gave virtually identical results. Figure 5 (b) shows a comparison of the results from the distributed parameter simulation model and the proposed analytical frequency-domain model. As can be seen, the analytical and simulated results agree very well. It shows that the analytical models are effective for predicting the four-port SIHS characteristics, given the above assumptions.
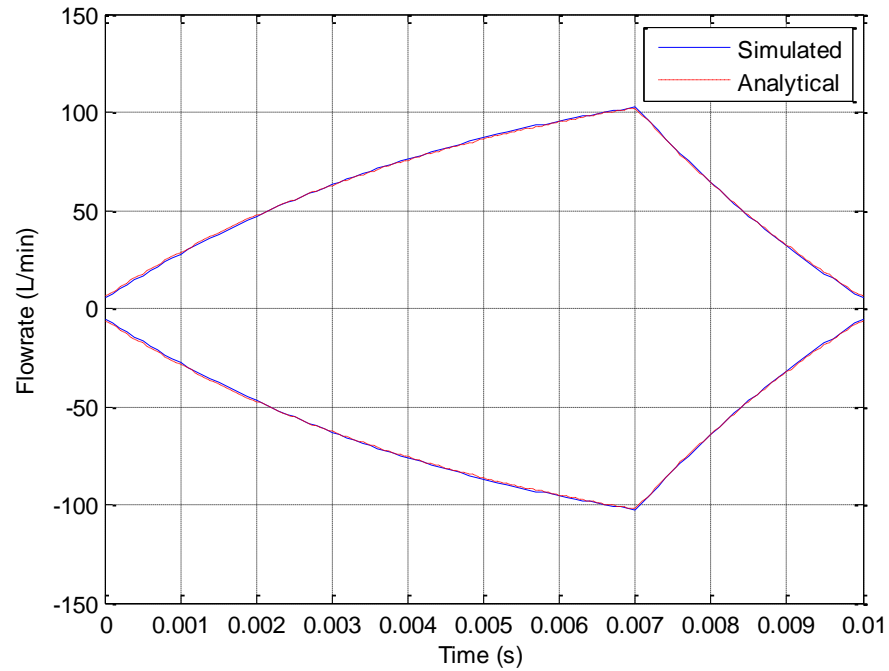
(a) lumped parameter model
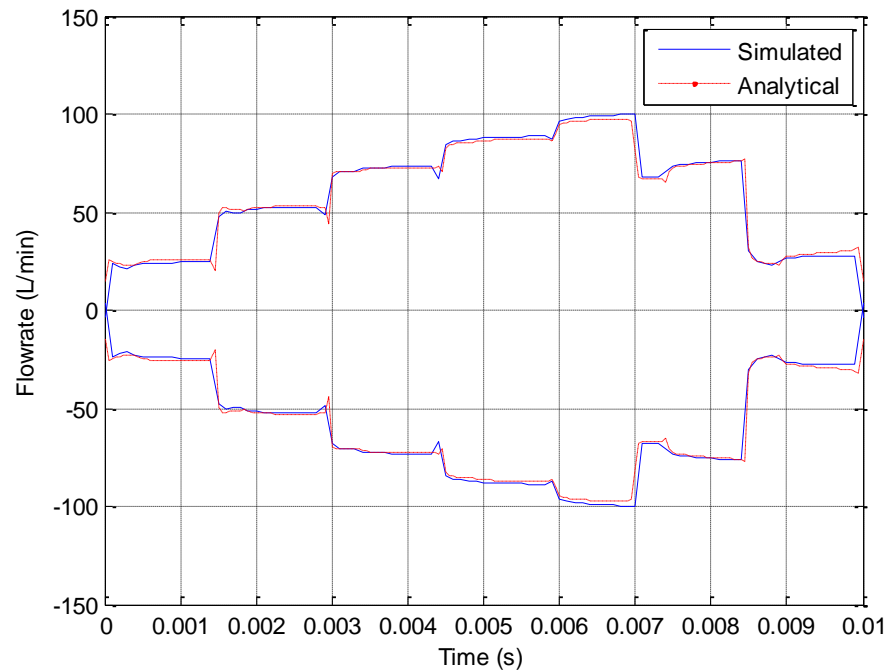
(b) distributed parameter model

Fig. 5: Comparison of dynamic flow rates $q_1(t)$ and $q_2(t)$ using the analytical and the simulated models

Figure 6 shows the results by using equation (10), (22) and (14) to demonstrate the flow loss and pressure loss. The flow loss is represented by using lumped and distributed parameter models, respectively. The wave propagation effect, which strongly influences system efficiency and can be used for system optimisation [8, 9], can be seen clearly in the above figure.
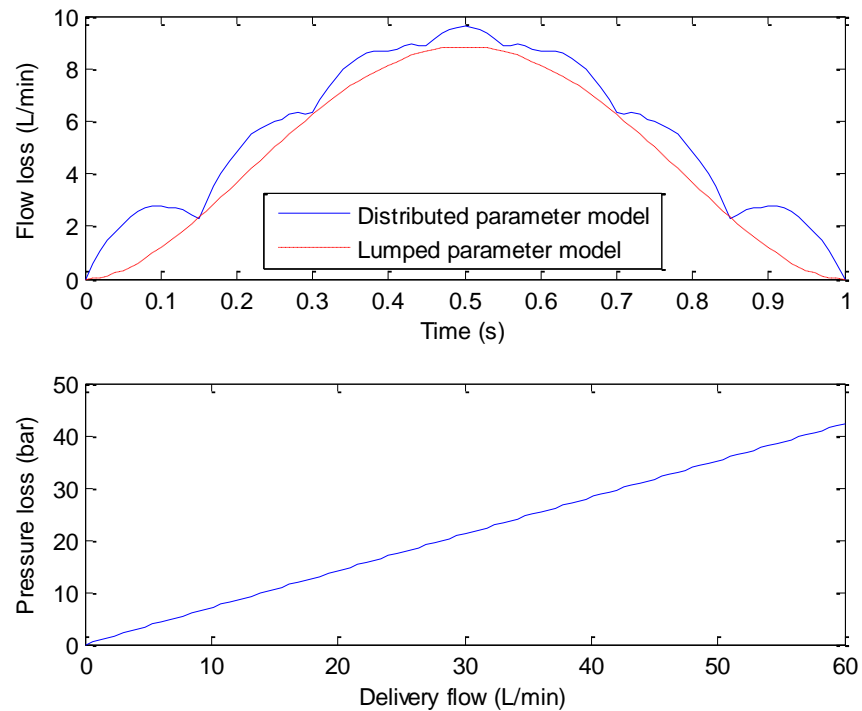

Fig. 6: Flow loss and pressure loss of the four-port SIHS

Figure 7 shows system efficiency contours (in percent) and pressure-flow characteristics for different ratio settings from 0 to 1. The top-left and bottom-right quadrants represent negative or over-running load. Low efficiency occurs with a very low delivery flowrate at different switching ratios, because the flow losses become dominant. As the analytical model is based on the assumption of a linear valve resistance, the pressure-flow characteristics curves are linear in this case. Compared with the previous results obtained by using Simulink models published in [1], the proposed models correctly and accurately predicted system characteristics and physical trends.
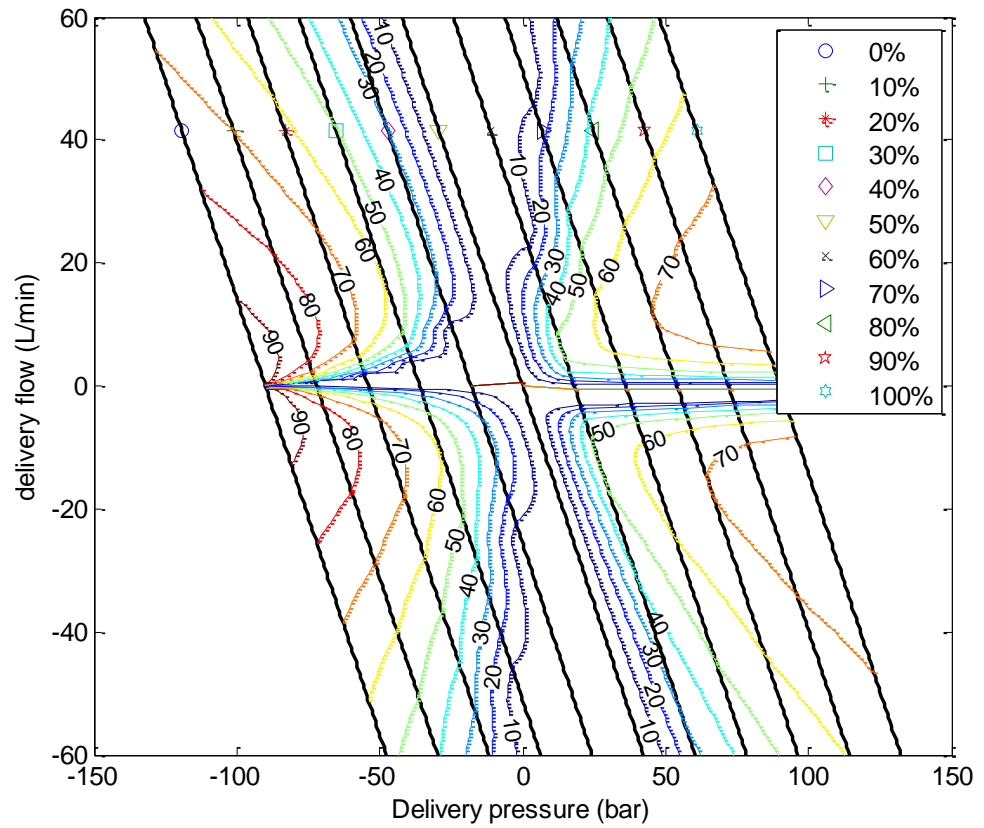
Fig. 7: Pressure-flow characteristics and efficiency of a four-port SIHS

The power losses of the four-port valve configuration are compared with the three-port SIHS (same parameters were used), as shown in Figure 8. The power loss of the four-port valve configuration is about twice that of the three-port SIHS. The shape and trends of the power loss are similar for these two configurations. It is inferred that the optimization procedure for the three-port valve SIHS can be applied for the optimization of the four-port valve configuration. Regarding the control flexibility, the four-port configuration is versatile for more applications, like a four-port valve.
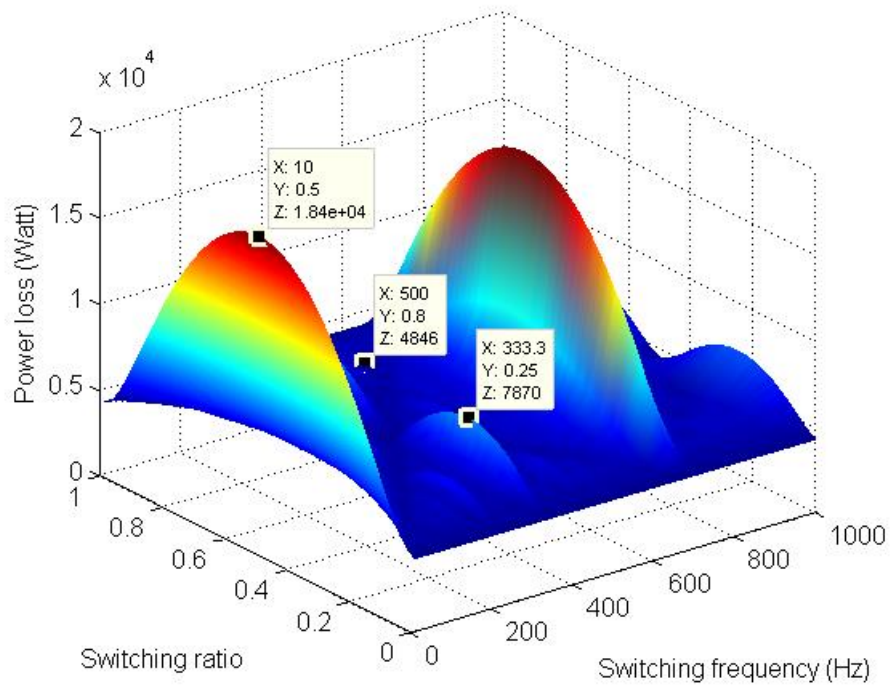
(a) Four-port configuration
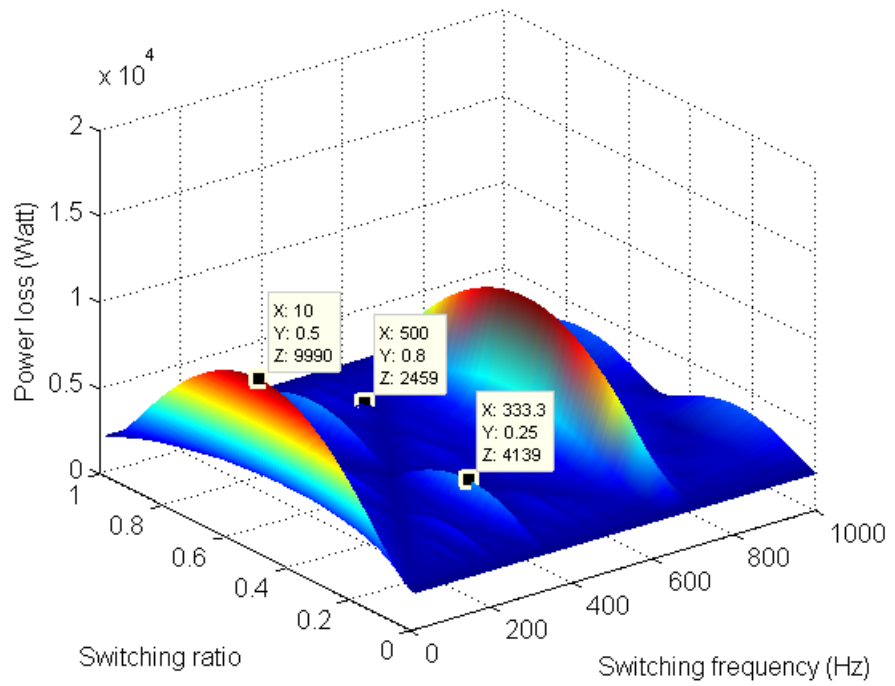
(b) Three-port configuration

Fig.8: Comparison of system power loss of a SIHS in a four-port and three-port configuration

6 DISCUSSIONS AND CONCLUSIONS

Analytical models for investigating the four-port SIHS based on a lumped parameter model and a distributed parameter model have been found to agree well with numerical simulations. The analytical and simulated results show that the analytical models are effective for investigating and analyzing the characteristics and performance of a four-port SIHS. Also, the analytical models have been found to be reliable and effective, and are much faster to run than the time domain numerical simulations. They can be used to aid in the design and optimization of a four-port SIHS.

The four-port SIHS has the advantages of control flexibility and versatility of use compared with the SIHS in a three-port configuration, providing true four-quadrant operation and regeneration. However it has more power loss and flow loss. These advantages and disadvantages are similar to those of a four-port modulating valve.

There is considerable work still to be done to investigate the performance of a four-port SIHS through experiments, and including the consideration of non-linearities, dynamics of the high-speed switching valve and losses that occur in the switching transition period and leakage. An analytical distributed parameter model for a four-port SIHS including the valve non-linearity, switching transition dynamics and leakage, similar to a previous model for a three-port valve [9], will be studied in future work.

ACKNOWLEDGEMENTS

REFERENCES

[1]   Johnston, D.N., "A switched inertance device for efficient control of pressure and flow," *Bath/ASME Fluid Power and Motion Control Symposium*, Hollywood, USA, pp.1-8. 2009.

[2]   Brown, F.T., "Switched reactance hydraulics: a new way to control fluid power," *Proc. National Conference on Fluid Power, Chicago,* Feb-Mar, pp.25-34, 1987.

[3]   Scheidl, R., Manhartsgruber, B and Winkler, B., "Hydraulic switching control – principles and state of the art," *The First Workshop on Digital Fluid Power, Tampere, Finland*, 2008.

[4]   Winkler, B. and Scheidl, R., "Development of a fast seat type switching valve for big flow rates", *The Tenth Scandinavian International Conference on Fluid Power*, Tampere, Finland. 2007.

[5]   Van de Ven, J. and Katz, A., "Phase-shift high-speed valve for switch-mode control," *Journal of Dynamic Systems, Measurement, and Control*. Vol.133. 2011.

[6]   Kudzma, S., Johnston, D.N., Plummer, A., Sell, N., Hillis, A. and Pan, M., "A high flow fast switching valve for digital hydraulic systems," *The 5th Workshop on Digital Fluid Power, Tampere, Finland*, 2012.

[7]   Scheidl, R., Manhartsgruber, B. and Kogler, H., "Mixed time-frequency domain simulation of a hydraulic inductance pipe with a check valve" *Proceedings of the*

Institution of Mechanical Engineers, Part C: Journal of Mechanical Engineering Science.vol.225, pp. 2413-2421. 2011.

[8]   Pan, M., Johnston, D. N., Plummer, A., Kudzma, S., Hillis, A.J., Theoretical and experimental studies of a switched inertance hydraulic system. Proceedings of the Institution of Mechanical Engineers, Part I, Journal of Systems and Control Engineering. Vol. 228 Issue 1, pp. 12-25, 2014.

[9]   Pan, M., Johnston, D. N., Plummer, A., Kudzma, S., Hillis, A.J., Theoretical and experimental studies of a switched inertance hydraulic system including switching transition dynamics, non-linearity and leakage. Proceedings of the Institution of Mechanical Engineers, Part I, Journal of Systems and Control Engineering. vol. 228 no. 10, pp. 802-815, 2014.

[10]   Pan, M., Robertson, J., Johnston, D. N., Plummer, A., Hillis, A.J., Experimental investigation of a switched inertance hydraulic system. Bath/ASME Symposium on Fluid Power and Motion Control, Bath, September 10-12, 2014.

[11]   De Negri, V.J., Wang, P., Plummer,A. and Johnston, D.N., "Behavioural prediction of step-up switched-inertance hydraulic control systems," International Journal of Fluid Power, Volume 15, Issue 1, 2014, 1-9

[12]   Brown, F.T., Tentarelli, S.C., Ramachandran, S., "A hydraulic rotary switched inertance servo-transformer, " Journal of Dynamic Systems, Measurement, and Control, vol. 110, pp.144-150, 1988.

[13]   Akers, A., Gassman,M. and Smith, R., "Hydraulic power system analysis," CRC Press, 2006.

[14]   Wang, P., Kudzma, S., Johnston, D.N., Plummer, A., Hillis, A.J., "The influence of wave effects on digital switching valve performance," *The Fourth Workshop on Digital Fluid Power*, Linz, Austria, 2011.

[15]   Johnston, D.N., "Measurement and prediction of the fluid borne noise characteristics of hydraulic components and systems." *PhD Thesis, University of Bath.* 1987.

[16]   Stecki, J.S and Davis, D., "Fluid transmission lines—distributed parameter models part 1: A review of the state of the art." *Proceedings of the Institution of Mechanical Engineers, Part A: Journal of Power and Energy*. vol. 200, pp.215-228,1986.

[17]   Krus, P., Weddfelt, K. and Palmberg, J.O., "Fast pipeline models for simulation of hydraulic system." *Journal of Dynamic Systems, Measurement, and Control*, vol. 116, pp.132-136, 1994.

[18]   Johnston, D.N., "The transmission line method for modelling laminar flow of liquid in pipelines." *Proceedings of the Institution of Mechanical Engineers, Part I: Journal of Systems and Control Engineering*, pp. 1-12.2012.

[19]   Johnston, D.N., "An enhanced transmission line method for modelling laminar flow of liquid in pipelines." *to be submitted to Proceedings of the Institution of Mechanical Engineers, Part I: Journal of Systems and Control Engineering*, 2013.

NOMENCLATURE

c	Speed of sound
d	Tube internal diameter
f	Switching frequency
I	Tube inertance
J_0, J_1	Bessel functions of the first kind of orders zero and one
j	Imaginary unit
L	Tube length
n	Number of harmonics
P_n	Fourier coefficient of pressure
p_d	Delivery pressure
p_i	Inlet pressure
p_{loss}	Pressure loss
p_H	High supply pressure
p_L	Low supply pressure
Δp	Pressure drop
Q_n	Fourier coefficient of flowrate
q	Flowrate
q_a	Initial flowrate during the rising phase
q_b	Initial flowrate during the falling phase
q_d	Average delivery flowrate
q_H	Steady state flowrate from the high pressure supply port
$\bar{q}_H$	Average flowrate from the high pressure supply port
q_L	Steady state flowrate from the low pressure supply port
$\bar{q}_L$	Average flowrate from the low pressure supply port
q_{loss}	Flow loss
R	Overall resistance of the system
R_t	Resistance of the inertance tube
R_v	Resistance of the high-speed switching valve
T	Switching cycle
t	Time
$V_{ab}, V_{a'b'}$	Flow volume during the period $0 \leq t \leq \alpha T$
$V_{bc}, V_{b'c'}$	Flow volume during the period $\alpha T < t \leq T$
P_{loss}	System power loss
Z_0	Pipe characteristic impedance
Z_E	Entry impedance
α	Switching ratio
η	System efficiency
ν	Kinematic viscosity
ρ	Density
ξ	Viscous wave correction factor
τ	Time constant
ω	Radian frequency